Australian Earthquake Engineering Society
2023 National Conference, 23-25 November 2023
Brisbane, Queensland, Australia

Informing Seismic Hazard with Geodesy & Remote-Sensing from Türkiye to Central Asia

Tamarah King[1]

1. COMET (The Centre for Observation and Modelling of Earthquakes, Volcanoes and Tectonics), Department of Earth Sciences, University of Oxford

(Now: Community Safety Branch, Geoscience Australia, Jerrabomberra Ave and Hindmarsh Drive, Symonston, Canberra, 2609)

Abstract

COMET (The Centre for Observation and Modelling of Earthquakes, Volcanoes and Tectonics) uses satellite measurements alongside ground-based observations and geophysical models to study active faults and earthquakes. This paper provides an overview of COMET research products in Türkiye and Central Asia, where interseismic deformation and active faults are evident. It also touches on how these products highlight the complexity and difficulty of seismic hazard modelling in Australia.

Three COMET datasets will be discussed, which each contribute to seismic hazard models. Researchers at COMET have and continue to pioneer INSAR methods including co-seismic interferograms and time-series modelling. For example, the Türkiye (Türkiye) INSAR strain-rate map directly estimates strain-accumulation across faults, while the LICSAR portal and satellite cross-correlation methods are used to quantify co-seismic and post-seismic deformation (including after the devastating 2023 Türkiye-Syria earthquake).

Similar methods are applied in the Tien Shan, where active faults are identifiable in satellite imagery and elevation data, but rates of activity are uncertain and expensive to obtain through field work. Here COMET and GEM (the Global Earthquake Model) are collaborating to produce block-model-informed PSHA inputs using active fault databases, GNSS (Global Navigation Satellite Systems), and INSAR.

While these methods are useful in tectonically active regions, they serve to highlight the difficulties facing Australian seismic hazard modelling where similar methods cannot be used due to low (to unobservable) tectonic strain and very long earthquake recurrence on known faults.

Keywords: seismic hazard, geodesy, active faults, INSAR, Türkiye, Central Asia, Australia.

1 Introduction

This paper provides an overview of how geodetic and remote-sensing data can inform and improve seismic hazard models (e.g., PSHA). These data are most applicable at plate-boundary locations (e.g., Türkiye / Turkey), and have proven useful in zones of distributed tectonic strain (e.g., Central Asia). Unfortunately, the data and methods are not applicable for earthquake hazard in Australia and some other so-called 'Stable Continental Regions' due to incomparable tectonic strain rates, which will be explored at the end of this paper.

The movement of tectonic plates relative to each other produces an increase in strain across faults in the vicinity of the active plate boundary (Figure 1). Strain may be distributed within tens, hundreds, or thousands of kilometres from the plate boundary, depending on geological and geophysical conditions. In the upper crust this is typically released through earthquakes (e.g., elastic rebound theory (Reid, 1910), Figure 1).

For faults that are 'locked' (not creeping), strain accumulates during the interseismic period which may be hundreds to thousands of years in active tectonic locations. This may equate to centimetres per year (for plate boundary faults) or millimetres per year (for distributed active faults). Even mm/year signals are measurable through modern geodesy which allows quantitative measurements and modelling of the 'slip deficit' across a fault or region.

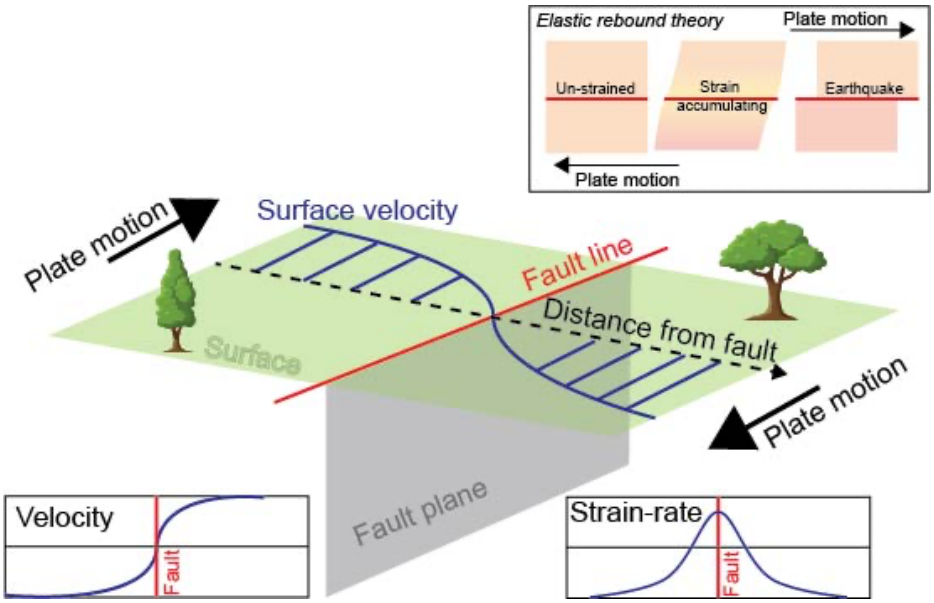

Figure 1: Schematic representation of how tectonic plate motion relates to surface velocities and strain accumulation across an active fault. Inset shows a schematic representing elastic rebound theory, the concept for why earthquakes occur due to the build up of tectonic strain across a fault.

One of the globally applicable issues with modelling seismic hazard is a short record of instrumental seismicity. Even regions with long written records of >M6.0 earthquakes (e.g., 700 years in China) have catalogue completeness issues below magnitudes ~4.0 due to the relatively short instrumental period (e.g., <100 years). By directly measuring strain-rate across a region or fault, the rate of expected seismicity can be modelled based on the amount of accumulating strain, providing constraints for seismic hazard assessments (Bird and Kreemer, 2015).

In addition to geodetic data, remote-sensing imagery of increasingly high resolution has proven useful for the detection and characterisation of active faults in the landscape. Fault databases are one of the primary inputs to seismic hazard models and while the locations of faults can be mapped remotely, field work is traditionally required to quantify rupture/recurrence characteristics. In locations that are difficult or impossible to conduct field work (for political or

geographical reasons), geodetic data can provide constraints on the locations, slip-rate and geometries of active faults.

1.1 GNSS

GNSS (Global Navigation Satellite Systems) is the general name for satellite-based geopositioning systems providing services on a global basis (e.g., the United States' Global Positioning System [GPS]). GNSS ground stations provide centimetre level instantaneous accuracy of the 3-dimensional location of a point on the ground. A network of stations each continuously measuring can be used to detect millimetre scale differences in relative motion due to large-scale tectonic plate deformation, local-scale across-fault deformation, or other signals (e.g., ground water extraction). GNSS velocity vectors are often shown in a fixed reference frame, e.g., vectors from GNSS stations in Türkiye are typically shown relative to a reference frame defined by measurements in the tectonically-inactive Eurasia plate.

1.2 INSAR

INSAR (Interferometric Synthetic Aperture Radar) is a satellite technique capable of measuring small movements in the ground surface regardless of cloud/weather conditions or time of day. Coseismic interferograms are a common product of INSAR, which can map how the ground moved during an earthquake.

Unlike GNSS which only provides point-data and must be interpolated to produce a map of displacement or strain accumulation, INSAR images produce a spatially continuous map of deformation across large regions covered by the satellite data. However, each image only measures the movement towards or away from the satellite. Combining multiple images from different viewing angles can give us sensitivity to lateral and vertical deformation.

Over the last decade, INSAR data have been used to produce direct measurements of tectonic deformation by stacking thousands of satellite images from many years across a given region. This provides a map where each pixel represents velocity relative to a fixed point, and where relative differences in velocity can indicate accumulation of strain across an active fault.

1.3 COMET and Sentinel-1

COMET (https://comet.nerc.ac.uk/) is a UK-based research group working on the application of geodetic and remote-sensing products to active tectonics and volcanoes. COMET has been continually funded by the UK National Environmental Research Council since the early 2000s, providing expertise in satellite- and field-based research for active tectonics.

COMET work closely with the European Space Agency (ESA) who launched the Sentinel-1 INSAR satellite array in 2014 (Sentinel-1a) and 2016 (Sentinel 1b). Up until 2020 Sentinel-1 provided near-global coverage with a repeat time of 12 days. Sentinel-1b failed in late 2021, but Sentinel-1a continues to provide coverage over a reduced area until ESA launches Sentinel-1c (likely in late 2024).

Researchers at COMET have pioneered multiple advancements in the use of INSAR. This includes: developing the LICSAR platform to automate processing earthquake interferograms, volcano monitoring, and background interferograms from the vast amounts of Sentinel-1 data (Lazecký *et al.*, 2020); advancing correction and processing methods to account for common issues with INSAR data (e.g. atmospheric noise, ground surface snow and ice, etc) (Yu *et al.*, 2018; Sadeghi *et al.*, 2021; Maghsoudi *et al.*, 2022); and developing methods and tools (e.g. the LICSBAS platform) to produce strain-rate maps across broad geographical regions (e.g. Türkiye, the Tibetan Plateau, the Tian Shan Mountains) (Morishita *et al.*, 2020; Weiss *et al.*, 2020; Maghsoudi *et al.*, 2022; Wright *et al.*, 2023).

2 Geodetic constraints on seismic hazard in Türkiye

2.1 Tectonic background

Türkiye sits between three major tectonic plates: the Arabian, African, and Eurasian. Tectonic movement is mostly accommodated through earthquakes and fault-creep along two major faults, the North Anatolian and East Anatolian Faults (Figure 2) (Aktug *et al.*, 2016). The rest of the strain is accommodated through a network of active faults throughout the country.

Despite a long written record of large damaging earthquakes (e.g. the 1513 M7.4 Gölbaşı earthquake), and a relatively high number of paleoseismic studies (Emre *et al.*, 2018), Türkiye still faces issues common to all seismic hazard modelling: poor earthquake catalogue completeness below ~M5.0, a deficit of dense paleoseismic investigations of all faults, and poorly resolved potential for multi-fault interactions during earthquake sequences (e.g. the 2023 Kahramanmaraş earthquake doublet (Karabulut *et al.*, 2023)).

2.2 INSAR Strain-rate models and fault slip-rate estimates

Figure 2, from Weiss *et al.* (2020), shows a large-scale (~800,000 km^2) velocity and strain-rate map produced using time-series INSAR data. This was the first such map to be produced, building off processing improvements made by the COMET group. This was made possible by comprehensive and repeating Sentinel-1 coverage with good overlap between ascending and descending data over a five-year period.

In total, the map is composed of a grid of 40 squares (250 km x 250 km) each including data from ~600-800 interferograms (i.e. 1200-1600 individual images) (Weiss *et al.*, 2020). These individual interferograms are stacked, processed, and stitched to produce a regional coherent model of displacements with a pixel size of approximately 1km. GNSS point-data are used to tie the model to a fixed reference frame (Eurasia), which allows the velocity and strain-rate within Anatolia to be derived relative to a fixed point (Weiss *et al.*, 2020).

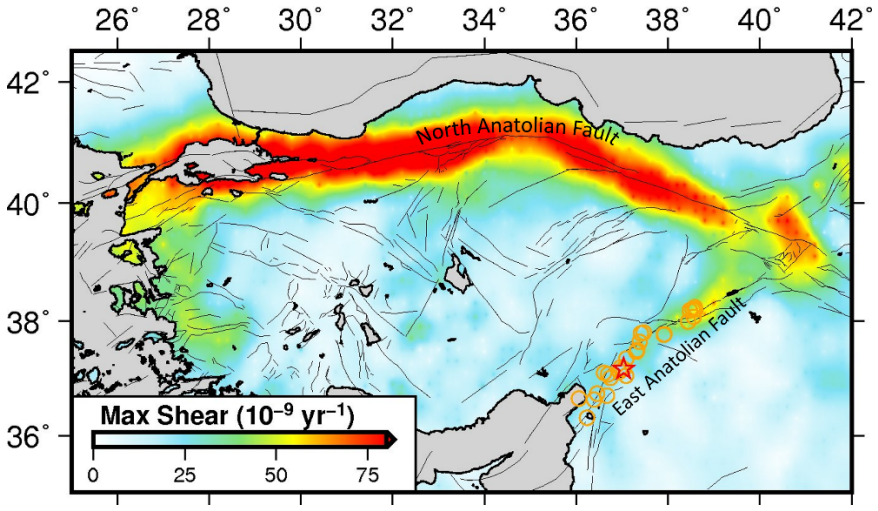

Figure 2: Map of strain-rate shown in nanostrain/year[1], derived from INSAR and GNSS data modelling. The location of the February 6th 2023 Mw 7.8 Kahramanmaraş earthquake is shown as a red star and aftershocks (up to 9 am UCT February 6th – not including the Mw 7.6 doublet event) are shown as orange circles. Mapped active faults are shown as grey lines. Map from Figure 4 of Weiss et al. (2020), modified and shared by T. Wright on February 6th 2023 on Twitter.com (https://twitter.com/timwright_leeds/status/1622530895163846656)

[1] Nanostrain is a dimensionless unit equivalent to 0.001 microstrain. 1 microstrain is equivalent to 1 mm change in a 1 km (1,000,000 mm) baseline.

The resulting strain-rate map (Figure 2) shows the distribution of strain across Türkiye, highlighting the main tectonic structures (the North Anatolian and East Anatolian Faults) and many minor active faults. This strain-rate map is viewable and interrogatable through the COMET website (https://comet.nerc.ac.uk/comet-lics-portal-velocities/). These data also highlights regions of ground water changes (e.g. agricultural extraction) (Weiss *et al.*, 2020).

Slip-rate estimates across active faults can be derived by extracting velocity profiles from the INSAR strain-rate map (Figure 3) (Hussain *et al.*, 2018; Weiss *et al.*, 2020). Slip-rate is calculated based on the relative difference in velocity across the active fault.

These profiles can also be used to estimate the 'locking depth' of the fault (i.e., fault width/depth) (Figure 3) which is useful for estimating maximum earthquake magnitude on a given fault. These parameters are one of the primary inputs into PSHA, and the INSAR strain-rate maps can densify the number of quantified estimates for any given fault or location.

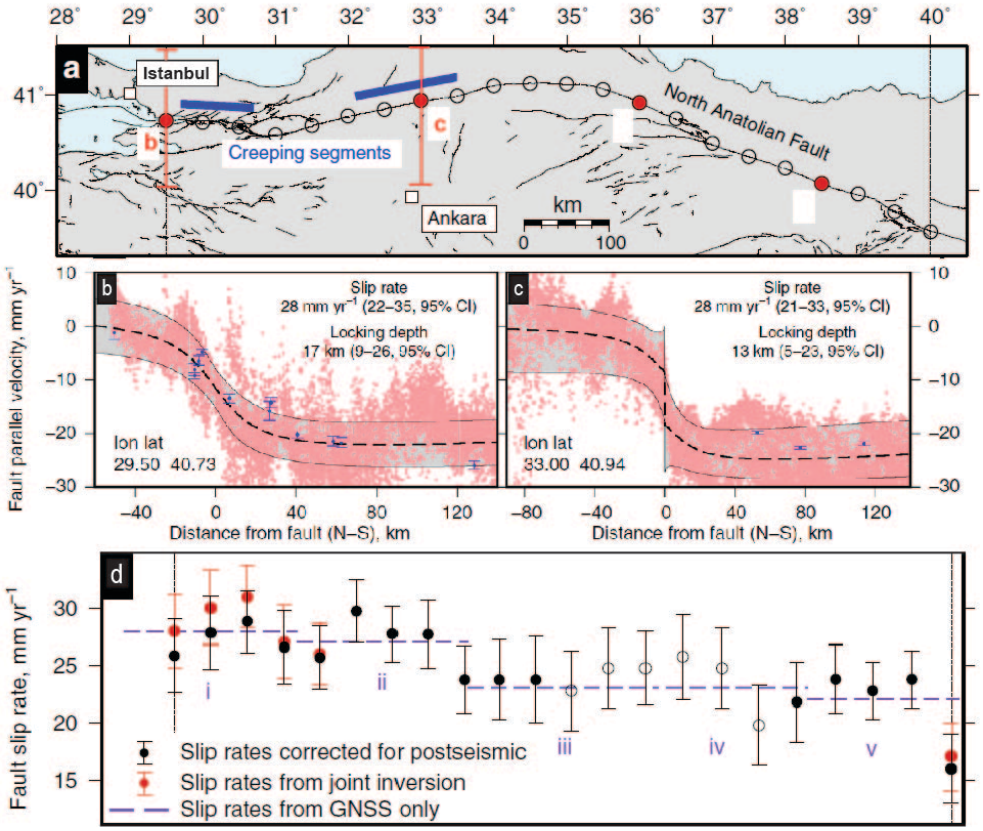

Figure 3: (a) map showing the North Anatolian Fault including locations of creeping sections, and the locations of profiles showing in (b), (c) and (d). (b) across fault velocity profiles through the INSAR derived data, with modelled slip-rate and locking-depth. Red dots are INSAR velocity data, blue dots are GNSS velocities. The step indicates a change in velocity due to strain accumulation across the North Anatolian Fault. (c) as with (b) but for a creeping section of the fault. Creeping sections continually release strain, creating a sharp step in velocity rates. (d) along-fault INSAR-derived slip-rates along the North Anatolian Fault. Map and graphs from figures 2 and 3 of Hussain et al. (2018).

In contrast to paleoseismic slip rates which require expensive and complicated trenching and/or geomorphic dating, INSAR time-series strain-rate maps can be used to extract slip-rates along the full length of a fault (Figure 3). These are particularly useful where variability in along-fault slip-rate may be present (e.g. Faure Walker *et al.* (2019)).

These INSAR derived slip-rate data should still be used with caution, as the uncertainties can be large and geodetic data will not represent long-term changes in slip-rate, which are commonly observed in paleoseismic investigations (e.g. Clark *et al.* (2012); Faure Walker *et*

al. (2021); Clark *et al.* (2022)). However, for very large faults (e.g., plate-boundary faults) which accommodate large amounts of strain, the assumption that geodetic rates match paleoseismic rates is generally valid.

2.3 Quantifying co-seismic displacements with INSAR and satellite imagery

Large and/or very shallow earthquakes have the potential to cause permanent surface deformation across a seismogenic fault. INSAR has been used to detect and quantify coseismic surface offsets since the mid-1990's, and the broad coverage and freely available data from Sentinel-1 program has allowed for a rapid expansion in the number of users of this data (Elliott *et al.*, 2020). The COMET LICSAR project (Lazecký *et al.*, 2020) automates the production of INSAR interferograms over every earthquake above a particular magnitude and depth threshold, making all data freely downloadable (https://comet.nerc.ac.uk/comet-lics-portal-earthquake-event/).

To date, the LICSAR system has been triggered fourteen times across Türkiye, highlighting the country's high rate of large-magnitude earthquakes and high seismic hazard. This includes the 2023 Kahramanmaras earthquake doublet (Figure 4). These data are acquired and processed quickly by the LICSAR system once the Sentinel satellite passes over the area (e.g., within four days for the 2023 earthquake). These support emergency response, and provide long-term understanding of the expected displacements, multi-fault interactions, and extent of damage surrounding known active faults. These insights and data directly contribute to PFDHA (probabilistic fault displacement hazard assessment).

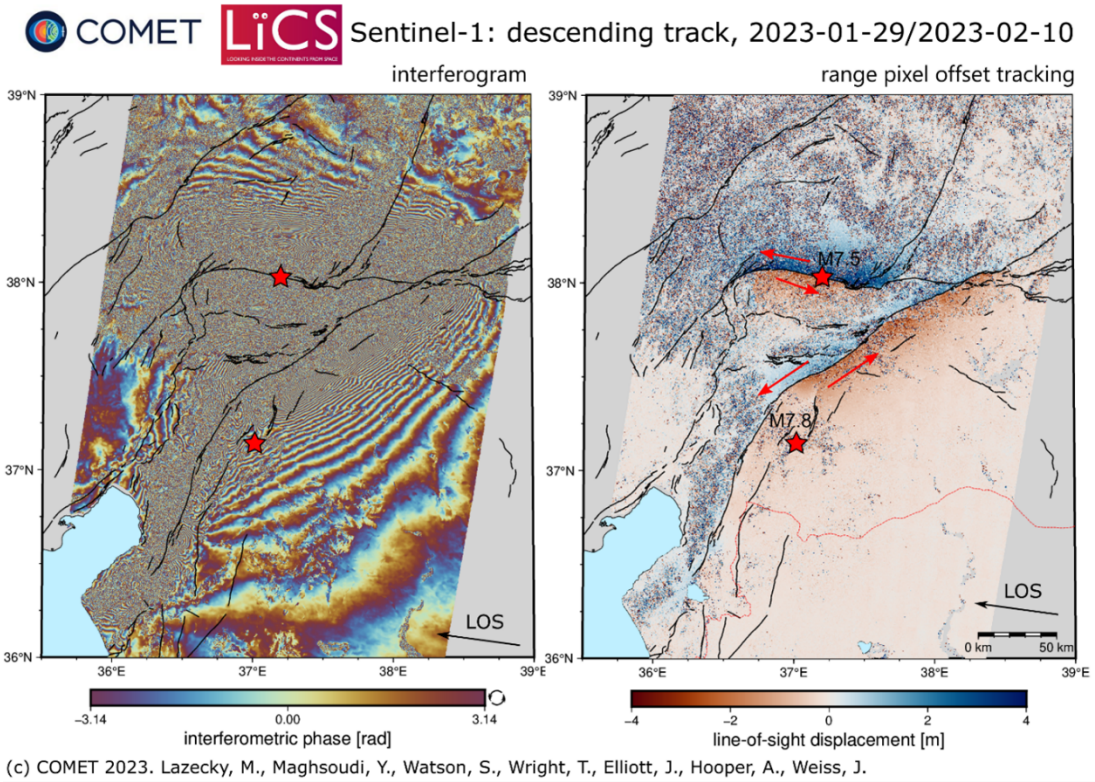

Figure 4: (a) Coseismic INSAR wrapped interferogram for the 2023 Kahramanmaras earthquake doublet. Each repeating fringe of colours represents approximately 2.8 cm of permanent ground displacement (up to 6 m total) (b) unwrapped interferogram using pixel tracking showing the total LOS displacement along a combined ~400 km of fault rupture. Active faults are shown as black lines. Maps from COMET (https://comet.nerc.ac.uk/turkiye-syria-earthquakes-february-2023/)

Following production of the Türkiye strain-rate map, the COMET group has produced strain-rate maps over broad areas of Central Asia including the Tibetan Plateau and the Tien Shan

Mountains (Figure 5). In addition to this, as background work the LICSAR processor produces interferograms of overlapping Sentinel-1 data continually for use across multiple applications (active tectonics, ground water monitoring, etc). In total the portal includes 1.4 million interferograms, with ~40 thousand being added each month.

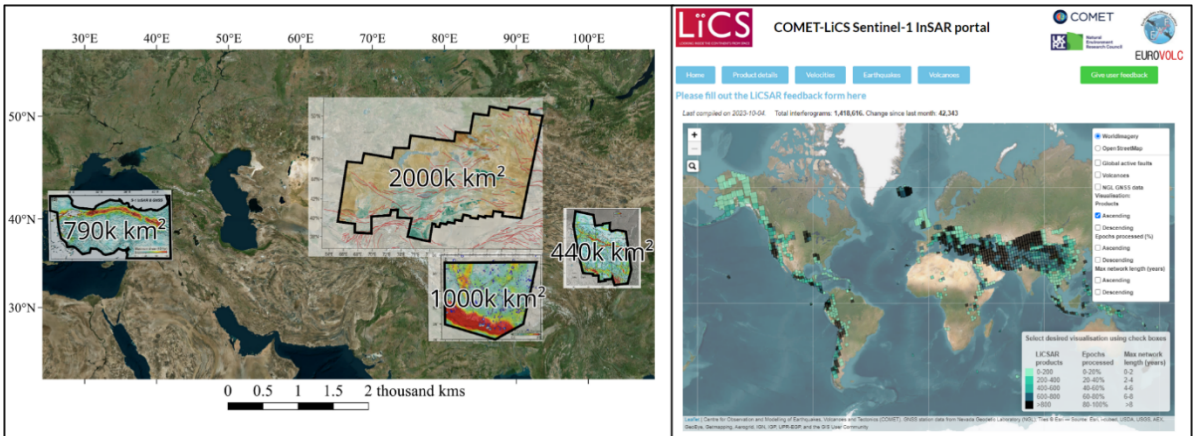

Figure 5: (a) Current extent of COMET INSAR time-series strain-rate maps including: Türkiye (Weiss et al., 2020); North Eastern Tibetan Plateau (Maghsoudi et al., 2022); Central Tibetan Plateau (Wright et al., 2023); and the Tien Shan (unpublished: Ou, et al. 2023). (b) the LICSAR portal (https://comet.nerc.ac.uk/comet-lics-portal/) showing the distribution of available background interferograms. Note that New Zealand is obscured but is thoroughly covered by background interferograms. No background interferograms have been processed for Australia.

3 Geodetic constraints on seismic hazard in the Tien Shan

3.1 Tectonic background

The Tien Shan Mountains stretch across Kyrgyzstan and parts of Kazakhstan, China, Uzbekistan*, and Tajikistan* (*depending on some but not all geographic definitions).

This region is considered ‘intraplate’, but unlike Australia (also considered ‘intraplate’), the earthquakes and active faulting are directly related to tectonic strain from the Indo-Eurasian collision, a large collisional plate boundary beneath the Himalayan mountains.

Long-term GNSS recording shows that the Indian and Eurasian plates converging at ~60mm/year, with ~40mm/year taken up by Himalayan faults (Zubovich *et al.*, 2010). The rest of the convergence (~20mm/year) is mostly accommodated by active faults in the Tien Shan (Zubovich *et al.*, 2010), despite these faults being ~1000km north of the ‘plate boundary’. In contrast, similarly long-term GNSS recordings in Australia have yet to measure strain accumulation across the continent, despite being much closer to the nearest plate boundary on the northern edge of Australia. This is due to large differences in the types of plate boundaries and associated geophysical properties.

The Tien Shan Active Fault Database (King *et al.*, 2021), which encompasses an area of 1000 x 400 km (approximately the size of New South Wales), contains approximately 133 major faults of between 10 – 850 km length (Figure 6). Over half of these faults show evidence of surface rupturing earthquakes since the last glacial period (approx. 12ka), and are capable of earthquakes up to M8.0-8.5 (e.g. Tsai *et al.* (2022)).

Due to the large number of faults, and a relatively ‘moderate’ strain rate (where ‘high’ might be Türkiye, and ‘low’ might be Australia), any one fault has a long recurrence interval (in the order of thousands of years, e.g., Tsai *et al.* (2022)). This region also has a poor earthquake catalogue of completeness for the instrumental period. This creates issues for seismic hazard modelling where the historic earthquake catalogue alone cannot be relied upon to accurately locate active faults or their maximum magnitude earthquakes over long timeframes.

These earthquake catalogue and active-fault data issues create complications for seismic hazard modelling, which are similar to the complications facing Australian seismic hazard models. Unlike Australia however, geodetic data can play a role in bridging the gap between paleoseismology and earthquake catalogues.

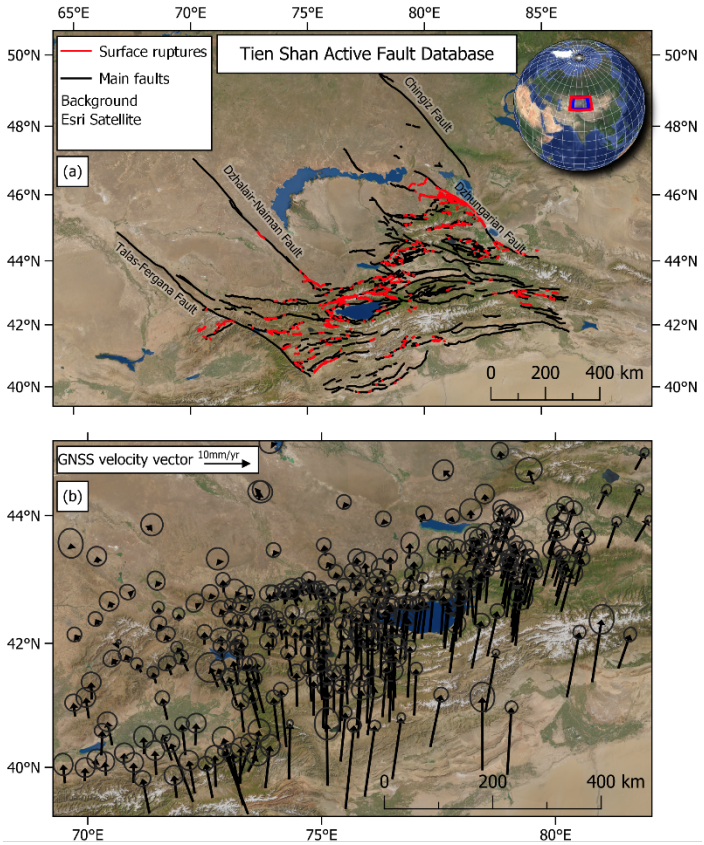

Figure 6: (a) Map of the Tien Shan Active Fault Database (King et al., 2021). Black lines are mapped active faults, red lines are mapped historic earthquakes ruptures or paleoseismic surface ruptures (b) GNSS velocities compiled by C. Rollins (GNS/COMET) from various sources. Vectors represent the velocity for each individual GNSS site relative to stable Eurasia. Large changes in velocity across the Tien Shan from south to north indicate that faults are actively accumulating strain. Arrowhead ellipses represent the east and north measurement uncertainties for each point.

3.2 Block Modelling for seismic hazard inputs

The Tien Shan Active Fault Database provides an accurate representation of the locations of active faults across the Tien Shan, mapped predominately from satellite-derived imagery and topography data. While the location of active faults is useful, other parameters (e.g., slip-rate, fault-length, fault-dip, down-dip width, and rupture behaviour) are necessary to include these faults as seismic sources in seismic hazard models.

Quantifying the rates of earthquakes and the geometry (e.g., dip) of faults in this region is difficult. Traditional field-based paleoseismic investigations are complicated by political, geographical, and cost issues.

In the absence of a dense paleoseismic database of slip-rates and geometries, COMET and the Global Earthquake Model (GEM) team have been collaborating to use tectonic block-models to derive reasonable slip-rate estimates. These models use the fault database to constrain the edges of each ‘block’, and GNSS and/or paleoseismic data to constrain the velocities of each ‘block’ through time (Styron, 2022). Differences in block velocities produce

'strain buildup' along block-interfaces (i.e., faults), which can be resolved into modelled slip-rates on each fault. See Figure 6 on page 15 of Styron (2022) for modelled results for the Tien Shan (https://www.authorea.com/doi/full/10.1002/essoar.10512747.1).

In addition to this block modelling, the COMET team are currently finalising an INSAR strain-rate map across the entire Tien Shan (draft version shown in Figure 5). This map will help to constrain the locations of active faults, and provide velocity constraints where GNSS data are sparse and/or difficult to obtain.

While there are many issues and assumptions to block modelling methods, the integration of fault databases and geodetic data provide useful estimates of PSHA inputs which are otherwise unobtainable for the region.

4 Potential for Application to Australia

4.1 Undetermined strain

As outlined above, Australia faces similar challenges to the Tien Shan in modelling seismic hazard, where the short earthquake catalogue may poorly represent past and future hazard due to long recurrence intervals. Unlike the Tien Shan, where strain is observably accumulating on faults due to a known tectonic plate boundary collision, geodetic data (specifically GNSS data) have yet to identify any accumulating strain across the Australian continent or individual faults (above the uncertainty of the measurements).

The rate and magnitude of earthquakes in Australia has been used as a proxy for strain rate (Braun *et al.*, 2009). The maximum strain rate found using this method was between 3×10^{-9} – 30×10^{-9} / year. This is equivalent to between white (5×10^{-9}/year) and green (~40×10^{-9}/year) on the INSAR derived Türkiye strain rate map (Figure 2). This should be geodetically measurable strain, which raises the question of why the earthquake-derived rate produces such a large modelled strain-rate, while geodetic monitoring fails to identify strain across a similar region. This is an as-yet underexplored geological and geophysical problem.

4.2 Active fault mapping

The moderately high strain rate and longevity of active faulting in the Tien Shan (approx. 10 Ma (Li *et al.*, 2022)), mean satellite-based fault databases (e.g. King *et al.* (2021)) can accurately capture the locations of hazardous earthquake sources. These faults leave tectonic geomorphic markers such as uplifted topography and offset/deformed drainages, alluvial fans, glacial deposits, and other young geomorphic features.

While hundreds of potentially and known active faults have been mapped across Australia Clark (2012), the recurrence rate on many of these faults is likely orders of magnitude longer (e.g. 10,000 – 100,000 years) than those in the Tien Shan (e.g. 1,000 years) which are themselves considered 'long' by paleoseismologists working in plate-boundary regions. This means the remote identification of faults is difficult and uncertain in Australia, and there are no remote tools (e.g., geodetically informed block modelling) to help quantify the rate of activity on mapped faults. Paleoseismic field work is required to constrain any single fault's potential seismic hazard, and even this is complicated by Australia's long-lived geomorphic stability and often undatable surface sediments / geomorphic features.

5 Conclusion

Modern geodetic methods (GNSS and INSAR) are capable of measuring rates of tectonic strain in actively deforming regions, which can provide key parameters for seismic hazard modelling. Satellite derived data can support seismic hazard modelling across very large geographical areas through the mapping of faults (imagery and topographic data) and quantification of fault slip-rates and dip (INSAR and GNSS). These methods are limited to locations where tectonic rates of deformation are high enough to produce a signal. No geodetically measured strain rates are available for Australia, which raises fundamental

questions about how Australian earthquakes and active faults fit into standard geological models for earthquake occurrence. This highlights one of the reasons why long-term Australian seismic hazard is difficult to understand and quantify relative to active plate boundary settings.

6 References

Aktug, B., Ozener, H., Dogru, A., Sabuncu, A., Turgut, B., Halicioglu, K., Yilmaz, O., and Havazli, E. (2016). Slip rates and seismic potential on the East Anatolian Fault System using an improved GPS velocity field, *Journal of Geodynamics* Vol 94-95, pp 1-12, 10.1016/j.jog.2016.01.001.

Bird, P., and Kreemer, C. (2015). Revised Tectonic Forecast of Global Shallow Seismicity Based on Version 2.1 of the Global Strain Rate Map, *Bulletin of the Seismological Society of America* Vol 105, No 1, pp 152-166, 10.1785/0120140129.

Braun, J., Burbidge, D. R., Gesto, F. N., Sandiford, M., Gleadow, A. J. W., Kohn, B. P., and Cummins, P. R. (2009). Constraints on the current rate of deformation and surface uplift of the Australian continent from a new seismic database and low-T thermochronological data, *Australian Journal of Earth Sciences* Vol 56, No 2, pp 99-110, 10.1080/08120090802546977.

Clark, D. (2012). *Neotectonic Features Database*, Canberra, Australia, Geoscience Australia, Commonwealth of Australia, pp.

Clark, D., Griffin, J., La Greca, J., Quigley, M., Sellmann, S., Ninis, D., Kuang, K., and Wilson, A. (2022). Large earthquake recurrence on the Willunga Fault, South Australia, *Australian Earthquake Engineering Society National Conference*, Mount Macedon, Victoria, Australia.

Clark, D., McPherson, A., and Van Dissen, R. J. (2012). Long-term behaviour of Australian stable continental region (SCR) faults, *Tectonophysics* Vol 566-567, pp 1-30, 10.1016/j.tecto.2012.07.004.

Elliott, J. R., de Michele, M., and Gupta, H. K. (2020). Earth Observation for Crustal Tectonics and Earthquake Hazards, *Surveys in Geophysics* Vol 41, pp 1355–1389, 10.1007/s10712-020-09608-2.

Emre, Ö., Duman, T. Y., Özalp, S., Şaroğlu, F., Olgun, Ş., Elmacı, H., and Çan, T. (2018). Active fault database of Turkey, *Bulletin of Earthquake Engineering* Vol 16, No 8, pp 3229-3275, 10.1007/s10518-016-0041-2.

Faure Walker, J., Paolo, B., Bruno, P., Gerald, R., Lucilla, B., Scotti, O., Visini, F., and Peruzza, L. (2021). Fault2SHA Central Apennines database and structuring active fault data for seismic hazard assessment, *Nature Scientific Data* Vol 8, No 87, pp 1-20, 10.1038/s41597-021-00868-0.

Faure Walker, J. P., Visini, F., Roberts, G., Galasso, C., McCaffrey, K., and Mildon, Z. (2019). Variable fault geometry suggests detailed fault-slip-rate profiles and geometries are needed for fault-based probabilistic seismic hazard assessment (PSHA), *Bulletin of the Seismological Society of America* Vol 109, No 1, pp 110-123, 10.1785/0120180137.

Hussain, E., Wright, T. J., Walters, R. J., Bekaert, D. P. S., Lloyd, R., and Hooper, A. (2018). Constant strain accumulation rate between major earthquakes on the North Anatolian Fault, *Nat Commun* Vol 9, No 1, pp 1392, 10.1038/s41467-018-03739-2.

Karabulut, H., Güvercin, S. E., Hollingsworth, J., and Konca, A. Ö. (2023). Long silence on the East Anatolian Fault Zone (Southern Turkey) ends with devastating double earthquakes (6 February 2023) over a seismic gap: implications for the seismic potential in the Eastern Mediterranean region, *Journal of the Geological Society* Vol 180, No 3, 10.1144/jgs2023-021.

King, T. R., Elliott, A., Styron, R., and Walker, R. (2021). *COMET Central Asia Fault Database*, Retrieved 09/10/2023, from https://comet.nerc.ac.uk/comet-central-asia-fault-database/.

Lazecký, M., Spaans, K., González, P. J., Maghsoudi, Y., Morishita, Y., Albino, F., Elliott, J., Greenall, N., Hatton, E., Hooper, A., Juncu, D., McDougall, A., Walters, R. J., Watson, C. S.,

Weiss, J. R., and Wright, T. J. (2020). LiCSAR: An Automatic InSAR Tool for Measuring and Monitoring Tectonic and Volcanic Activity, *Remote Sensing* Vol 12, No 15, 10.3390/rs12152430.

Li, W., Chen, Y., Yuan, X., Xiao, W., and Windley, B. F. (2022). Intracontinental deformation of the Tianshan Orogen in response to India-Asia collision, *Nat Commun* Vol 13, No 1, pp 3738, 10.1038/s41467-022-30795-6.

Maghsoudi, Y., Hooper, A. J., Wright, T. J., Lazecky, M., and Ansari, H. (2022). Characterizing and correcting phase biases in short-term, multilooked interferograms, *Remote Sensing of Environment* Vol 275, 10.1016/j.rse.2022.113022.

Morishita, Y., Lazecky, M., Wright, T., Weiss, J., Elliott, J., and Hooper, A. (2020). LiCSBAS: An Open-Source InSAR Time Series Analysis Package Integrated with the LiCSAR Automated Sentinel-1 InSAR Processor, *Remote Sensing* Vol 12, No 3, 10.3390/rs12030424.

Reid, H. F. J. R. o. t. R. S. C., Carnegie Institution, Washington, DC (1910). The mechanism of the earthquake, the California earthquake of April 18, 1906, Vol 2, pp 16-18.

Sadeghi, Z., Wright, T. J., Hooper, A. J., Jordan, C., Novellino, A., Bateson, L., and Biggs, J. (2021). Benchmarking and inter-comparison of Sentinel-1 InSAR velocities and time series, *Remote Sensing of Environment* Vol 256, 10.1016/j.rse.2021.112306.

Styron, R. (2022). Contemporary Slip Rates of All Active Faults in the Indo-Asian Collision Zone (Pre-print), *ESS Open Archive* Vol, 10.1002/essoar.10512747.1.

Tsai, C. H., Abdrakhmatov, K., Mukambayev, A., Elliott, A. J., Elliott, J. R., Grützner, C., Rhodes, E. J., Ivester, A. H., Walker, R. T., and Wilkinson, R. (2022). Probing the Upper End of Intracontinental Earthquake Magnitude: A Prehistoric Example From the Dzhungarian and Lepsy Faults of Kazakhstan, *Tectonics* Vol 41, No 10, 10.1029/2022TC007300.

Weiss, J. R., Walters, R. J., Morishita, Y., Wright, T. J., Lazecky, M., Wang, H., Hussain, E., Hooper, A. J., Elliott, J. R., Rollins, C., Yu, C., González, P. J., Spaans, K., Li, Z., and Parsons, B. (2020). High-Resolution Surface Velocities and Strain for Anatolia From Sentinel-1 InSAR and GNSS Data, *Geophysical Research Letters* Vol 47, No 17, 10.1029/2020gl087376.

Wright, T. J., Houseman, G. A., Fang, J., Maghsoudi, Y., Hooper, A., Elliott, J., Lazecky, M., Ou, Q., Parsons, B. E., Rollins, C., Shen, L., and Wang, H. (2023). High-resolution geodetic strain rate field reveals dynamics of the IndiaEurasia collision, *EarthArXiv Preprint* Vol.

Yu, C., Li, Z., Penna, N. T., and Crippa, P. (2018). Generic Atmospheric Correction Model for Interferometric Synthetic Aperture Radar Observations, *Journal of Geophysical Research: Solid Earth* Vol 123, No 10, pp 9202-9222, 10.1029/2017jb015305.

Zubovich, A. V., Wang, X. Q., Scherba, Y. G., Schelochkov, G. G., Reilinger, R., Reigber, C., Mosienko, O. I., Molnar, P., Michajljow, W., Makarov, V. I., Li, J., Kuzikov, S. I., Herring, T. A., Hamburger, M. W., Hager, B. H., Dang, Y. M., Bragin, V. D., and Beisenbaev, R. T. (2010). GPS velocity field for the Tien Shan and surrounding regions, *Tectonics* Vol 29, No 6, pp 1-23, 10.1029/2010TC002772.